https://doi.org/10.3311/PPtr.42464

Periodica Polytechnica Transportation Engineering

Application of Finite Element Method to Study the Influence of Operation Conditions on Tire Performance

Vu Hai Quan[1*], Tam Tran Quang[1]

[1] Faculty of Automobiles, School of Mechanical and Automotive Engineering, Hanoi University of Industry, 298 Cau Dien Street, 120000 Hanoi, Vietnam
[*] Corresponding author, e-mail: quanvh@haui.edu.vn

Received: 11 October 2025, Accepted: 19 March 2026, Published online: 22 June 2026

Abstract

The paper presents the results of a study applying numerical simulation to investigate the effects of load, pressure and speed on the performance of Bridgestone Ecopia EP422 tires. The 3D model of the research object was built using Siemens NX software and analyzed using Ansys Workbench. The main output parameters including deformation, stress and contact area were analyzed under various operating conditions. The results show that load directly affects the contact area; low pressure increases the contact area but reduces fuel efficiency; high speed reduces contact time and causes stress concentration at the sidewall. The simulation results are consistent with previous experimental studies, confirming the reliability of the model and its applicability in tire design and optimization. The topic opens up the potential for integrating advanced factors such as material nonlinearity, environmental impact and artificial intelligence in subsequent studies.

Keywords

temperature tire, Bridgestone Ecopia, structure tire, working conditions

1 Introduction

Automobile tires play a decisive role in transmitting forces between the vehicle and the road surface. The mechanical properties of tires, including stiffness, load-carrying capacity and rolling resistance, directly affect the vehicle's performance, stability and fuel consumption (Sabey et al., 1970). As the automotive industry moves towards energy optimization and emission reduction goals, it is necessary to study the factors that affect tire performance.

The Bridgestone Ecopia EP422 Plus is a tire that aims to reduce rolling resistance and save fuel, through the use of new materials and optimized design. However, the actual performance of this tire depends not only on the design structure but is also significantly affected by operating conditions such as load, inflation pressure and speed (Hùng and Công, 2021). Quantifying the impact of these conditions on tire performance is necessary to properly evaluate the performance and optimize it in real-world operations.

Several previous studies have shown the relationship between operating conditions and tire performance. Specifically, Li et al. (2012) proposed a tire wear prediction model based on the analysis of the effects of load, speed and temperature. The model showed the ability to accurately reflect the wear phenomenon over time and under different operating conditions. In Vietnam, experimental studies by Dang and Le (2018) evaluated tire durability according to QCVN 34:2017/BGTVT standard (The Government of Electronic Information Portal, 2017), clearly identifying the effects of load and speed on tire size deviation and deformation (Dang and Le, 2018). However, these studies often only consider each factor individually and have not integrated numerical simulation in the overall assessment of the simultaneous influence of many different parameters.

In this study, a numerical simulation model based on the Finite Element Method (FEM) is used to analyze the simultaneous effects of tire pressure, load and speed on performance (Lv et al., 2023) with the Bridgestone Ecopia EP422 tire as an example. The evaluation parameters include total deformation, contact pressure distribution and contact area at the rolling surface. The objective of the study is to clarify the influence of each factor and the correlation between them, thereby providing recommendations to manufacturers and suitable operating conditions for this type of tire (Sahu and Kanchwala, 2024).

Cite this article as: Hai Quan, V., Tran Quang, T. (2026) "Application of Finite Element Method to Study the Influence of Operation Conditions on Tire Performance", Periodica Polytechnica Transportation Engineering, https://doi.org/10.3311/PPtr.42464

This study uses numerical simulation to quantitatively analyze the effects of three main operating factors: load, tire pressure, and speed on the performance of the Bridgestone Ecopia EP422 Plus tire. The analysis process is divided into two main stages. In the first stage, a tire structure model is established and analyzed using the finite element method under dynamic contact conditions with the road surface (Kislov et al., 2023). Next, characteristic mechanical quantities such as total deformation, pressure distribution, and contact area are extracted to investigate the changes in tire performance characteristics under different load and speed conditions, corresponding to real-life operating scenarios (Gong et al., 2024). The simulation results not only provide input data for evaluating tire performance under typical conditions, but also serve as a basis for proposing optimal operating limits for this type of tire.

2 Theoretical basis

2.1 Theoretical basis of tire dynamics

Consider a wheel in contact with the road surface and the wheel axle is attached to the vehicle frame, the characteristic parameters include: mass (m), moment of inertia (I), dynamic radius (r_d) (Persson, 2011). It is assumed that the vehicle does not oscillate vertically.

In the general case, the wheel is subjected to the following forces and moments (Selig et al., 2014):

- Torque M: active torque (creating traction) or braking torque;
- Impact force from the road surface: the total reaction force from the contact area between the wheel and the road surface is analyzed into two components:
  - Tangential force (F_x): parallel to the contact plane, in the direction of vehicle motion;
  - Normal force (F_z): perpendicular to the road surface, affects tire pressure on the road surface.

The specific location of these forces is shown in Fig. 1.

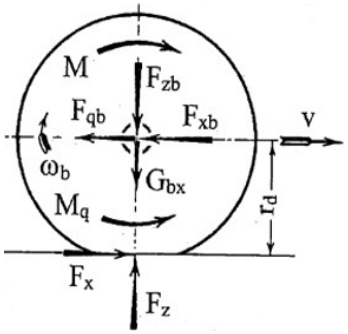

Fig. 1 Model of forces acting on the driving wheel

The force acting from the vehicle frame F_b is also divided into two components:

- Horizontal component F_{xb}: depends on the operating state of the wheel (passive, active or braking).
- Vertical component F_{zb}: is the static load of the vehicle distributed on the wheel, under non-oscillating conditions.

In addition, consideration should be given to:

- The weight of the wheel itself G_{bx}. Combined with F_{xb}, we have the total force from the frame:

$$G_b = F_{xb} + G_{bx}. \tag{1}$$

- Translational inertia force F_{qb}: arises due to vehicle acceleration; has the opposite direction to the motion when the vehicle accelerates and the same direction when the vehicle decelerates.
- Moment of inertia M_{qb}: corresponds to the rotational motion of the wheel under the influence of angular acceleration. When the vehicle moves uniformly, $F_{qb} = 0$ and $M_{qb} = 0$.

2.2 Theoretical basis of factors affecting tire performance

In traditional powertrains, the internal combustion engine (ICE) acts as the primary source of power, generating output torque, which is used to move the vehicle. This torque is generated by the combustion of the fuel and air mixture in the combustion chamber. When the mixture burns, the pressure generated from the combustion pushes the piston down to the bottom dead center during the explosion stroke. The piston then continues to perform the remaining cycles including exhaust, intake, and compression, forming a complete four-stroke cycle.

The up and down reciprocating motion of the piston is converted into rotary motion through the crankshaft. The output torque from the engine, denoted by T_{engine}, can be calculated by the expression (Suyabodha, 2017):

$$T_{\text{engine}} = \frac{\text{MEP} \cdot n_R}{2 \cdot n_R}, \tag{2}$$

where:

- MEP: mean effective pressure (Pa);
- V_d: engine working capacity (m^3);
- n_R: number of crankshaft revolutions per power cycle (for 4-stroke engines, $n_R = 2$).

The torque from the engine is then transmitted through the transmission system, which consists of the clutch and the gearbox (Grappe et al., 1999). The gearbox is responsible for adjusting the torque and rotational speed through different gears, ensuring that the vehicle can accelerate from rest to the design speed. The relationship between torque and rotational speed at the wheels is described by the expressions (Soica et al., 2020):

$$T_{\text{wheel}} = T_{\text{engine}} \cdot i_{\text{total}}, \tag{3}$$

$$n_{\text{wheel}} = \frac{n_{\text{engine}}}{i_{\text{total}}}, \tag{4}$$

where:

- T_{wheel}: torque at wheel (N·m);
- n_{engine}: engine rotation speed (rpm);
- n_{wheel}: wheel rotation speed (rpm);
- i_{total}: total transmission ratio of the transmission system.

For the wheels to rotate and propel the vehicle forward on a flat road surface, the torque generated must be sufficient to overcome the minimum resistance forces as shown in Fig. 2, including aerodynamic resistance R_d and rolling resistance R_r (Mukherjee, 2014). These forces are calculated using the following formulas:

$$R_d = \frac{1}{2} \cdot \rho \cdot C_d \cdot A \cdot v^2, \tag{5}$$

$$R_r = K_r \cdot W, \tag{6}$$

where:

- ρ: air density (kg/m^3);
- C_d: aerodynamic drag coefficient;
- A: front bumper area of the car (m^2);
- v: vehicle speed (m/s);
- K_r: tire rolling resistance coefficient;
- W: weight acting on the wheel (N).

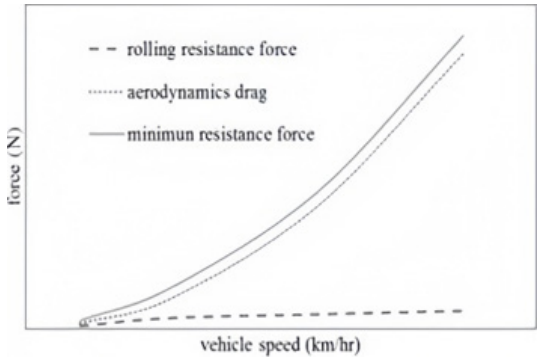

Fig. 2 Minimum resistance to driving at constant speed (Páscoa et al., 2012)

Rolling resistance is a force acting in the opposite direction of tire movement and depends on rolling speed, tire pressure, and rubber material properties. The mechanism of rolling resistance formation, shown in Fig. 3, originates from the asymmetrical stress distribution in the tire-road contact area, causing the resultant normal reaction force F_z to shift forward and generate a rolling resistance moment in the opposite direction of tire movement (Pillai, 2006).

3 Model building

A three-dimensional model of the Bridgestone Ecopia EP422 Plus tire, with the manufacturer's specifications as shown in Table 1, was built in Siemens NX (Siemens, 2024) (Fig. 4 (a) and (b)), and imported into ANSYS Workbench (ANSYS, Inc., 2025) for finite element analysis. ANSYS Workbench was chosen for its robust ability to handle

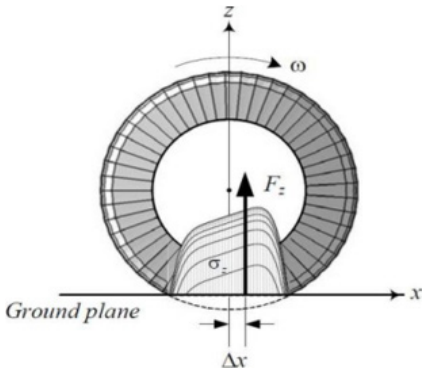

Fig. 3 Side view of tire stress distribution

Table 1 Technical specifications of Bridgestone Ecopia EP422 Plus tires (Bridgestone, 2025)

Detail	Information
Brand	Bridgestone
Seasons	Year round
Size	215/55R17
Load capacity	1,477 Pounds (670 kg)
Tread depth	10/32" (7.94 mm)
Tire aspect ratio	55.0
Speed rating	V
Ply rating	SL

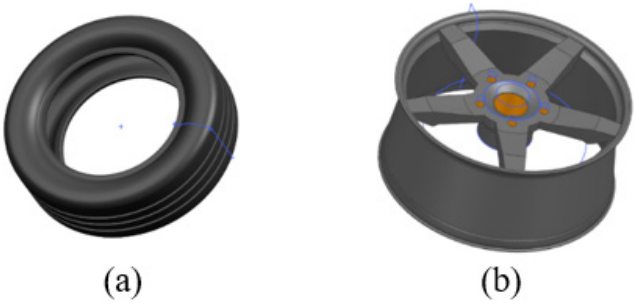

Fig. 4 Simulation model: (a) Tire model; (b) Rim model

nonlinear structural problems involving large deformations, material nonlinearity, and contact interactions – factors essential for accurately describing tire behavior under real-world operating conditions.

To ensure numerical accuracy and solution stability, a mesh convergence study was first performed. Three characteristic element sizes (20 mm, 15 mm, and 10 mm) were evaluated by comparing key output parameters such as deformation and contact characteristics. The results showed a significant improvement when reducing the element size from 20 mm to 15 mm, while further refinement to 10 mm led to negligible changes but substantially increased computational cost. Therefore, an element size of 15 mm was adopted for all subsequent simulations as an optimal compromise between accuracy and efficiency.

Based on the convergence analysis, the tire rubber domain was discretized using a MultiZone meshing strategy with structured hexahedral elements. This choice improves numerical robustness in large-deformation nonlinear analyses and minimizes element distortion in the contact region. The final tire model consisted of approximately 40,916 hexahedral elements. The rim was meshed using tetrahedral elements, while the road drum was discretized with hexahedral elements of the same characteristic size to ensure compatibility at the contact interface.

The mechanical behavior of the rubber was described using a Mooney–Rivlin hyperelastic material model, enabling realistic representation of the nonlinear elastic response under compression and rolling conditions. Other components, including body plies, bead wires, and the rim, were modeled as linear elastic materials with properties defined according to manufacturer data and published references.

The mechanical behavior of the rubber was described using a Mooney–Rivlin hyperelastic material model, which enables realistic representation of the nonlinear elastic response under compression and rolling conditions (Nguyen et al., 2023). The remaining components, including the tire plies, bead region, rim, and road surface, were modeled using material properties summarized in Table 2 (Haiquan et al., 2025; Quan et al., 2026).

Table 2 A short title for tables should be indented center

Material	Rubber	Body-ply	Bead wire	Concrete
Density (kg/m^3)	1,400	1,200	6,500	2,300
Poisson's ratio	–	0.3	0.3	0.18
Young's modulus (MPa)	–	500	207	30,000
Mooney–Rivlin constant (MPa)	C10 = 8.061	–	–	–
	C01 = 1.805	–	–	–
Thermal conductivity (W/m °C)	0.293	0.293	60.5	0.72
Hysteresis	0.1	–	–	–

4 Simulation results and discussion

4.1 Effect of load

In this study, the load applied to the tire was investigated at three values: 1 kN, 3 kN and 6 kN, while the tire pressure was kept constant at 35 psi (0.241 MPa), which is the standard value published by the manufacturer. The load range was chosen to simulate different operating conditions, from light to heavy loads, reflecting the real-life conditions that can occur when the vehicle is carrying few or many passengers and goods (Levesque et al., 2023). Keeping the tire pressure constant helps to isolate the effect of the load, thereby separately evaluating the impact of this parameter on the tire's performance and stress distribution. The selected load levels refer to published experimental data, providing a basis for comparison and verifying the reliability of the numerical simulation model used in the study (Ge et al., 2023).

The simulation results in Figs. 5 to 7 show that when the load acting on the tire increases from 1 kN to 6 kN,

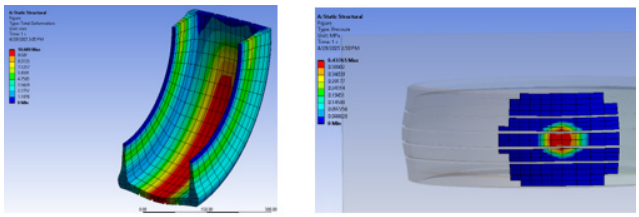

(a) (b)

Fig. 5 Simulation results at 1 kN: (a) Total deformation (mm); (b) Pressure at contact point (MPa)

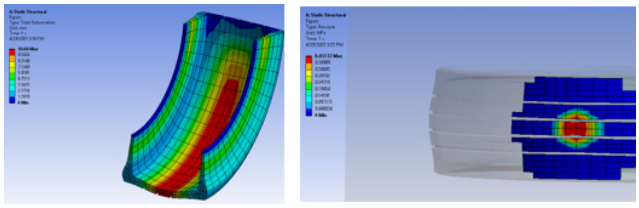

(a) (b)

Fig. 6 Simulation results at 3 kN: (a) Total deformation (mm); (b) Pressure at contact point (MPa)

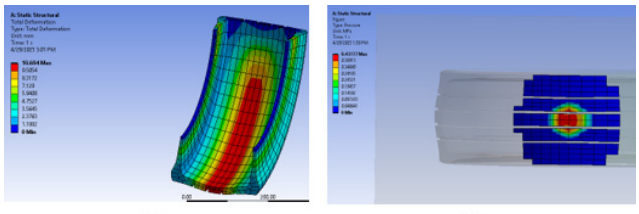

(a) (b)

Fig. 7 Simulation results at 6 kN: (a) Total deformation (mm); (b) Pressure at contact point (MPa)

the contact area between the tire and the road surface remains almost unchanged, fluctuating slightly between 5,428.9 mm^2 and 5,429.0 mm^2. This small variation reflects that the tire is still working in the linear elastic region, and the investigated load has not exceeded the nominal load capacity of the tire.

Specifically, the Bridgestone Ecopia EP422 tire is designed with a load index of 94, equivalent to a maximum load of 670 kg (~6.7 kN). Therefore, the load range from 1 to 6 kN corresponds to 15% to 90% of the limit load. In this range, the tire structure – including the plies and rim – still maintains a stable shape, without large deformations in the contact area.

However, as the load increases while the contact area remains unchanged, the average contact pressure across the contact surface increases significantly. This results in a more concentrated stress distribution, especially at the contact edge – the transition between the tread and the shoulder. As a result, the risk of localized wear, spot heating, and material degradation may increase if the tire is operated for a long time under high loading conditions.

Fig. 8 shows that the results obtained from the study tend to coincide with published experimental data (Ge et al., 2023), both in terms of the geometrical characteristics of the contact area and the degree of deformation under static loading conditions. This similarity shows that the finite element model correctly reflects the actual mechanical properties of the tire within the investigated load range. Thanks to that, the reliability of the simulation method as well as the accuracy of the entire research process are clearly confirmed.

From a design and operational perspective, this result shows that the tire structure has been optimized to maintain a stable geometry within the normal operating load range. However, when contact pressure increases under high load conditions, it is necessary to consider adjusting the inflation pressure or redistributing the load to limit the contact stress, thereby reducing the risk of local damage and extending tire life.

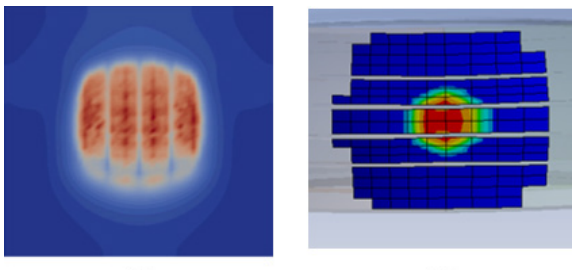

(a) (b)

Fig. 8 Comparison of numerical and experimental results: (a) Experimental results; (b) Simulation results

4.2 Effect of pressure

In this study, tire pressure was examined at 25 psi (0.172 MPa), 35 psi (0.241 MPa), and 45 psi (0.310 MPa). The central value of 35 psi, recommended by the manufacturer, represents the standard operating condition, while 25 psi and 45 psi simulate under- and over-inflation, which are frequently encountered in practice and can strongly influence tire safety and performance. This range was selected to assess the effect of deviations from the standard pressure, with reference to conditions reported in recent experimental studies (Norrby, 2012) to ensure consistency between simulation and experiment.

The simulation results in Figs. 9 to 11 indicate that the largest deformation area is concentrated at the tire bottom – the area that is in direct contact with the road surface and bears the main compressive load. Meanwhile, the edge and sidewall areas have smaller deformation levels because they are far from the main force transmission area and close to the fixed boundaries. The stress distribution shows that high stress does not appear at the contact area but is concentrated at the transition area between

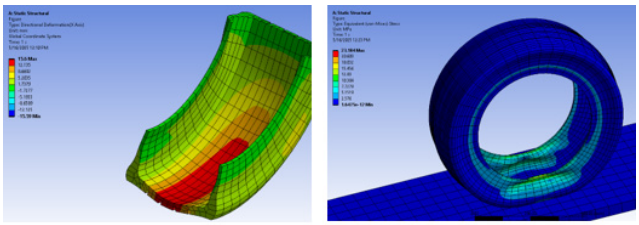

(a) (b)

Fig. 9 Simulation results at 25 psi (0.172 MPa): (a) Deformation (mm); (b) Stress distribution (MPa)

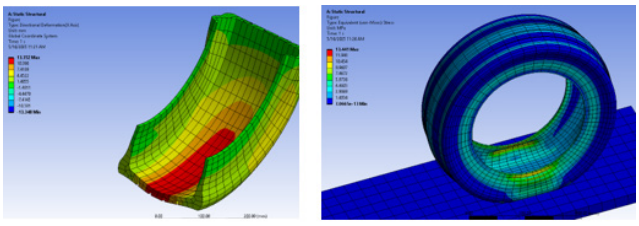

(a) (b)

Fig. 10 Simulation results at 35 psi (0.241 MPa): (a) Deformation (mm); (b) Stress distribution (MPa)

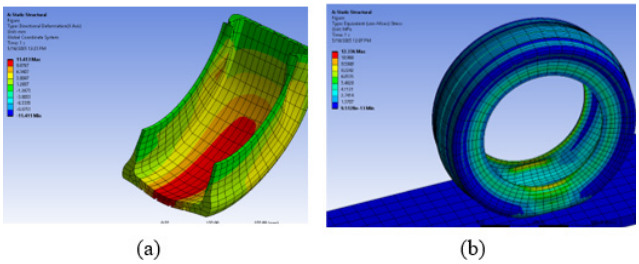

(a) (b)

Fig. 11 Simulation results at 45 psi (0.310 MPa): (a) Deformation (mm); (b) Stress distribution (MPa)

the rolling surface and the sidewall. The reason is that the combination of tension and bending caused by the curved shape of the tire when compressed leads to stress concentration in the area of sudden geometric change.

In addition, at the top of the tire, where there is no contact with the road surface, the stress is almost eliminated due to the large distance from the main bearing point. As the inflation pressure increases, the compression reaction at the bottom increases, increasing the stress level spread throughout the entire tire body, especially at the curved transition areas. This result shows that tire geometry and pressure play an important role in controlling the stress distribution and identifying potential damage risk areas.

When analyzing the simulation results in the first 1 s, Fig. 12 shows that the contact area between the tire and the road surface increases gradually over time at all three pressure levels investigated (25 psi, 35 psi and 45 psi). The rate of increase in contact area is inversely proportional to pressure: the tire inflated to 25 psi has the fastest increase rate, while one inflated to 45 psi has the slowest. At 1 s, the contact area reaches approximately 35,000 mm^2, 23,000 mm^2 and 20,000 mm^2, respectively, for the three pressure levels mentioned above.

The inverse relationship between tire pressure and contact area is explained based on the deformation properties of rubber materials. At low pressure, the tire is softer, deforming more easily under vertical load, resulting in an expanded contact area. Conversely, high pressure increases the tire stiffness, limiting the ability to deform, thereby reducing the contact area. Notably, at the highest pressure level (45 psi), a slight oscillation in the contact area appears in the range of 0.8 to 0.9 s. This phenomenon may be related to the rapid elastic response or natural vibration of the tire structure in the numerical simulation, reflecting the propagation of stress waves in the structure of a high-stiffness material.

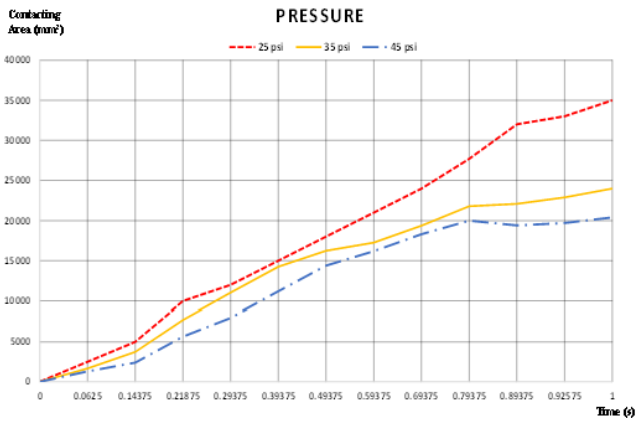

Fig. 12 Contact area in 1 s according to pressure values

The results obtained are consistent with the trends reported in previous studies. Specifically, the study by Norrby (2012) using the coast-down method showed that the rolling resistance increased by 48.52% at 25 psi and decreased by 13.46% at 45 psi compared to the standard level of 35 psi. At the same time, the study by Tomaraee et al. (2015) also showed that the rolling resistance increased linearly with the contact area between the tire and the ground. Thus, the simulation results in this study are not only mechanically consistent but also compatible with the experimental data, thereby confirming the reliability of the simulation model used.

4.3 Effect of speed

In this study, the tire speed range was investigated from 40 km/h to 100 km/h. This range was selected based on the common speed limit according to current regulations in Vietnam, in which the maximum speed allowed on highways often reaches 100 km/h. This speed range simultaneously represents three typical operating states of cars in real conditions: moving in residential areas (low speed), acceleration phase (medium) and stable traffic on highways (high speed). The investigation in this range allows to evaluate the influence of speed on the dynamic and mechanical properties of tires under typical operating conditions.

The simulation results Figs. 13 to 15 show that the area with the greatest deformation is still concentrated in the center of the tire bottom, where it is in direct contact with the road surface. When the vehicle moves, the weight of the entire system is pushed down to the contact surface, while the reactive force from the road surface creates a high local pressure area, leading to significant deformation at this location.

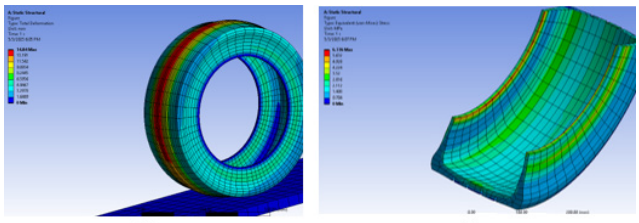

Fig. 13 Simulation results at 50 km/h: (a) Deformation (mm); (b) Stress distribution (MPa)

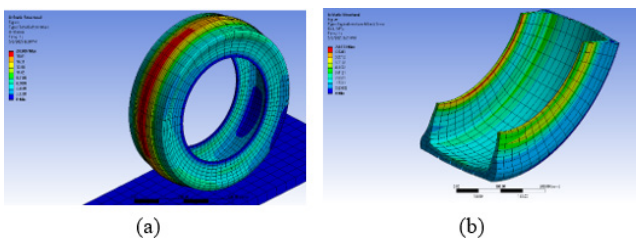

Fig. 14 Simulation results at 80 km/h: (a) Deformation (mm); (b) Stress distribution (MPa)

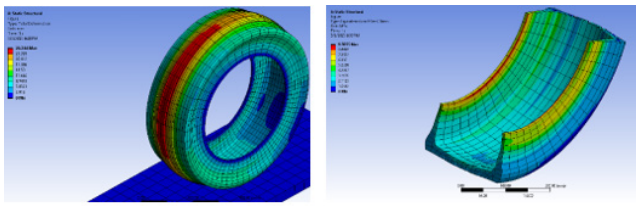

Fig. 15 Simulation results at 100 km/h: (a) Deformation (mm); (b) Stress distribution (MPa)

In addition to static compression, rotating tires are also affected by friction and inertia. Contact friction generates shear stress in the rubber surface, contributing to local shear deformation. As speed increases, the frequency and intensity of interaction between the tire tread and the road surface increase, generating more heat energy due to mechanical loss. Increased temperature leads to a decrease in material stiffness, thereby increasing the ability to deform in the main load-bearing area. Meanwhile, the sidewall edges have a smaller deformation because they are not directly affected by compression force and are less affected by contact friction.

Fig. 16 shows a tendency for contact area to decrease as speed increases, when analyzing the change in contact area over time at three speed ranges (50 km/h, 80 km/h and 100 km/h). Specifically, at 50 km/h, the contact area reaches its maximum value and continues to increase steadily until the end of the survey period. At 80 km/h, the contact area decreases slightly compared to 50 km/h and is almost stable after 0.8 s. At 100 km/h, the contact area is the smallest, changes insignificantly after 0.6 s and remains almost stable.

The mechanism of this trend can be explained based on the dynamic interaction between the tire and the road surface. As the speed increases, the time each point on the tire is in contact with the road surface is shorter, the rubber material has not had time to completely deform, resulting

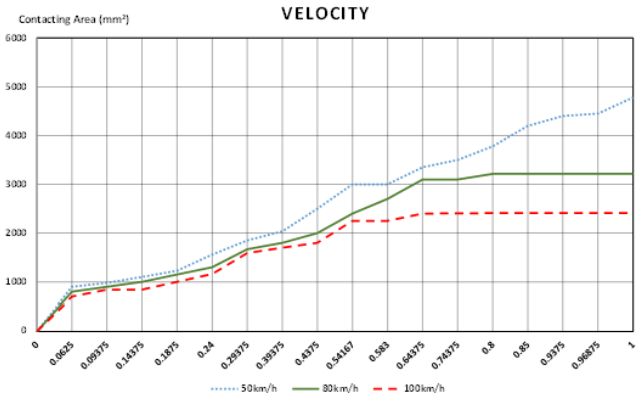

Fig. 16 Contact area in 1 s according to velocity values

in the contact area not expanding significantly. At the same time, the centrifugal force increases, causing the middle part of the tire to tend to expand outward, reducing the contact pressure at the bottom. In addition, friction at high speed generates heat, leading to an increase in temperature and pressure inside the tire according to the ideal gas law, making the tire more tense and reducing the ability to deform locally. As a result, at high speed, the tire maintains a stiffer shape, limiting the development of the contact area even though the load and contact time continue to increase.

4.4 Discussion

Through numerical simulation, this study analyzed the effects of load, pressure, and speed on the performance of the Bridgestone Ecopia EP422 tire. Under loads from 1–6 kN, the tire remained in the linear elastic region below its nominal limit (6.7 kN); however, the stable contact area caused a rise in contact pressure, which may lead to local heating and wear under prolonged use.

For pressure, the contact area decreased as inflation rose from 25 to 45 psi. Low pressure increased deformation and traction but also rolling resistance, while high pressure reduced deformation and cushioning. These results are consistent with earlier studies, confirming that maintaining the recommended 34–35 psi provides the best balance of grip, durability, and fuel efficiency.

At higher speeds (50–100 km/h), the contact area declined due to shorter ground contact, centrifugal bulging, and temperature-induced pressure rise. Stress concentration in the sidewall and transition zones highlighted the risk of fatigue or failure under severe conditions.

Overall, the findings show that tire behavior depends on the interplay of load, pressure, speed, and material properties. Operating within the optimal range of these factors is essential to ensure safety, service life, and efficiency. The results also demonstrate the usefulness of numerical simulation in predicting tire performance and supporting design optimization.

5 Conclusion

This study developed a numerical model to examine how load, pressure, and speed affect the performance of Bridgestone Ecopia EP422 Plus tires. Using a 3D model created in Siemens NX software (Siemens, 2024) and simulated in ANSYS Workbench (ANSYS, Inc., 2025), mechanical responses such as deformation, Von Mises stress, and contact area were evaluated. The findings indicate that load within the

elastic range mainly influences stress, low pressure increases deformation and contact area, while high speed reduces contact due to centrifugal force and higher internal pressure.

The results align with theoretical analysis and previous experiments, confirming the reliability of the proposed approach for tire mechanics. The model offers a foundation for selecting operating parameters and supporting tire design and optimization. Future work may incorporate nonlinear materials, dynamic loading, and machine learning to broaden its applicability in automotive engineering.

Acknowledgements

The authors would like to thank the School of Mechanical and Automotive Engineering, Hanoi University of Industry for providing the necessary equipment and materials to conduct the experiments and complete this research.

References

ANSYS, Inc. (2025) "ANSYS Workbench 2025, (Version 2025R1)", [computer program] Available at: https://www.ansys.com [Accessed: 20 March 2025]

Bridgestone (2025) "Ecopia EP422 Plus 215/55R17", [online] Available at: https://www.bridgestonetire.com/tire/ecopia-ep422-plus/215-55R17/ [Accessed: 10 October 2025]

Dang, V. H., Le, D. N. (2018) "Nghiên cứu, xác định độ bền lốp hơi ô tô bằng phương pháp thực nghiệm" (Research and determine the durability of car tires by experimental method), Transport Magazine, Sept. 20. [online] Available at: https://giaothong.tapchixaydung.vn/nghien-cuu-xac-dinh-do-ben-lop-hoi-o-to-bang-phuong-phap-thuc-nghiem-18365006.htm [Accessed: 10 October 2025] (in Vietnamese)

Ge, H., Quezada, J. C., Le Houerou, V., Chazallon, C. (2023) "Three-dimensional FEM–DEM coupling simulation for analysis of asphalt mixture responses under rolling tire loads", Construction and Building Materials, 369, 130615. https://doi.org/10.1016/j.conbuildmat.2023.130615

Gong, Z., Miao, Y., Lantieri, C. (2024) "Review of Research on Tire–Pavement Contact Behavior", Coatings, 14(2), 157. https://doi.org/10.3390/coatings14020157

Grappe, F., Candau, R., Barbier, B., Hoffman, M. D., Belli, A., Rouillon, J.-D. (1999) "Influence of tyre pressure and vertical load on coefficient of rolling resistance and simulated cycling performance", Ergonomics, 42(10), pp. 1361–1371. https://doi.org/10.1080/001401399185009

Haiquan, V., Thanh Tung, N., Anh Ngoc, N., Ngoc Minh, D. (2025) "Application of Finite Elements to Analysis of Side Collision Problems of Vehicle: A Case Nissan Rogue 2020 SUV Model", International Journal of Automotive Science And Technology, 9(1), pp. 81–88. https://doi.org/10.30939/ijastech..1581465

Hùng, T. M., Công, N. T. (2021) "Nghiên cứu ứng dụng phần mềm Ansys xác định độ bền lốp ô tô sử dụng tại Việt Nam" (Research on the application of ANSYS software to determining automobile tire durability in Vietnam, Transport and Communications Science Journal, 72(3), pp. 242–250. (in Vietnamese) https://doi.org/10.47869/tcsj.72.3.1

Kislov, V. M., Tsvetkova, Y. Y., Tsvetkov, M. V., Pilipenko, E. N., Salganskaya, M. V., Podlesniy, D. N., Zaichenko, A. Y., Salgansky, E. A. (2023) "Experimental Study of Gasification of Car Tires in Filtration Combustion with Different Heat Carriers", Combustion, Explosion, and Shock Waves, 59(2), pp. 199–205. https://doi.org/10.1134/S0010508223020107

Levesque, W., Bégin-Drolet, A., Lépine, J. (2023) "Effects of Pavement Characteristics on Rolling Resistance of Heavy Vehicles: A Literature Review", Transportation Research Record: Journal of the Transportation Research Board, 2677(6), pp. 296–309. https://doi.org/10.1177/03611981221145125

Li, Y., Zuo, S., Lei, L., Yang, X., Wu, X. (2012) "Analysis of impact factors of tire wear", Journal of Vibration and Control, 18(6), pp. 833–840. https://doi.org/10.1177/1077546311411756

Lv, T., Zang, L., Xue, C., Li, Y., Mao, Y., Wang, X. (2023) "Study on the Effect of Different Design Parameters of Sidewall Insert Rubber on the Mechanical Characteristics of Self-Supporting Run-Flat Tires", Lubricants, 11(11), 458. https://doi.org/10.3390/lubricants11110458

Mukherjee, D. "Effect of Pavement Conditions on Rolling Resistance", American Journal of Engineering Research (AJER), 3(7), pp. 141–148. [online] Available at: https://www.ajer.org/papers/v3(7)/R037141148.pdf [Accessed: 10 October 2025]

Nguyen, T.-C., Cong, K.-D. D., Dinh, C.-T. (2023) "Rolling Tires on the Flat Road: Thermo-Investigation with Changing Conditions through Numerical Simulation", Applied Sciences, 13(8), 4834. https://doi.org/10.3390/app13084834

Norrby, P. (2012) "Prediction of coast-down test results: A statistical study of environmental influences", MSc Thesis, Chalmers University of Technology. [online] Available at: https://publications.lib.chalmers.se/records/fulltext/160184.pdf [Accessed: 10 October 2025]

Páscoa, J. C., Brójo, F. P., Santos, F. C., Fael, P. O. (2012) "An innovative experimental on-road testing method and its demonstration on a prototype vehicle", Journal of Mechanical Science and Technology, 26(6), pp. 1663–1670. https://doi.org/10.1007/s12206-012-0413-8

Persson, B. N. J. (2011) "Rubber friction and tire dynamics", Journal of Physics: Condensed Matter, 23(1), 015003. https://doi.org/10.1088/0953-8984/23/1/015003

Pillai, P. S. (2006) "Inflation pressure effect on whole tyre hysteresis ratio and radial spring constant", Indian Journal of Engineering & Materials Sciences, 13, pp. 110–116. [online] Available at: https://nopr.niscpr.res.in/bitstream/123456789/7230/1/IJEMS%2013(2)%20110-116.pdf [Accessed: 10 October 2025]

Quan, V. H., Tam, T. Q., Duc, N. T., Quan, L. H., Hoa, T. P., Karpukhin, K. E. (2026) "Analysis of the influence of some factors on the temperature distribution and tire durability", Innovation in Engineering, 3(1), pp. 1–10. https://doi.org/10.58712/ie.v3i1.41

Sabey, B. E., Williams, T., Lupton, G. N. (1970) "Factors Affecting the Friction of Tires on Wet Roads", SAE Transactions, 79, pp. 1203–1218. [online] Available at: https://www.jstor.org/stable/44644490 [Accessed: 10 October 2025]

Sahu, G. N., Kanchwala, H. (2024) "Experimental modal analysis of a tire: an exploration of different operating and boundary conditions", Journal of the Brazilian Society of Mechanical Sciences and Engineering, 46(11), 667. https://doi.org/10.1007/s40430-024-05237-7

Selig, M., Lorenz, B., Henrichmöller, D., Schmidt, K., Ball, A., Persson, B. (2014) "Rubber Friction and Tire Dynamics: A Comparison of Theory with Experimental Data", Tire Science and Technology, 42(4), pp. 216–262. https://doi.org/10.2346/tire.14.420403

Siemens (2024) "Siemens Digital Industries Software, (NX 2024)", [computer program] Available at: https://www.siemens.com/vi-vn/ [Accessed: 02 March 2025]

Soica, A., Budala, A., Monescu, V., Sommer, S., Owczarzak, W. (2020) "Method of estimating the rolling resistance coefficient of vehicle tyre using the roller dynamometer", Proceedings of the Institution of Mechanical Engineers, Part D: Journal of Automobile Engineering, 234(13), pp. 3194–3204. https://doi.org/10.1177/0954407020919546

Suyabodha, A. (2017) "A Relationship between Tyre Pressure and Rolling Resistance Force under Different Vehicle Speed", MATEC Web of Conferences, 108, 12004. https://doi.org/10.1051/matecconf/201710812004

The Government of Electronic Information Portal (2017) "QCVN 34:2017/BGTVT Quy chuẩn kỹ thuật quốc gia về lốp hơi ô tô" (QCVN 34:2017/BGTVT National technical regulation on pneumatic tyres for automobiles), The Government of Electronic Information Portal, Hanoi, Vietnam. (in Vietnamese)

Tomaraee, P., Mardani, A., Mohebbi, A., Taghavifar, H. (2015) "Relationships among the contact patch length and width, the tire deflection and the rolling resistance of a free-running wheel in a soil bin facility", Spanish Journal of Agricultural Research, 13(2), e0211. https://doi.org/10.5424/sjar/2015132-5245